Modeling the Electrical Energy Discharged by Lightning Flashes Using Capacitors for Application with Lightning Datasets

Vicente Salinas,[a] Eric C. Bruning,[a] Edward R. Mansell,[b] and Matthew Brothers[c]

[a] *Atmospheric Science Group, Department of Geosciences, Texas Tech University, Lubbock, Texas*
[b] *NOAA/OAR/National Severe Storms Laboratory, Norman, Oklahoma*
[c] *NOAA/NWS, Cheyenne, Wyoming*

ABSTRACT: This study employed a parallel-plate capacitor model by which the electrostatic energy of lightning flashes could be estimated by considering only their physical dimensions and breakdown electric fields in two simulated storms. The capacitor model has previously been used to approximate total storm electrostatic energy but is modified here to use the geometry of individual lightning flashes to mimic the local charge configuration where flashes were initiated. The energy discharged may then be diagnosed without context of a storm's entire charge structure. The capacitor model was evaluated using simulated flashes from two storms modeled by the National Severe Storms Laboratory's Collaborative Model for Multiscale Atmospheric Simulation (COMMAS). Initial capacitor model estimates followed the temporal evolution of the flash discharge energy of COMMAS for each storm but demonstrated the need to account for an adjustment factor μ_c to represent the fraction of energy a flash dissipates, as this model assumes the entire preflash energy is discharged by a flash. Individual values of μ_c were obtained simply by using the ratio of the COMMAS flash to capacitor energy. Median values $\tilde{\mu}_c$ were selected to represent the flash populations for each storm, and were in range of $\tilde{\mu}_c = 0.019$–0.021. Application of $\tilde{\mu}_c$ aligned the magnitudes of the capacitor model discharge energy estimates to those of COMMAS and to those estimated in previous studies. Therefore, by considering a μ_c within range of $\tilde{\mu}_c$, application of the capacitor model for observed lightning datasets is suggested.

KEYWORDS: Atmospheric electricity; Convective storms; Energy budget/balance; Idealized models

1. Introduction

The energy discharged by lightning flashes have received interest both for the discharge itself (Wilson 1920; Malan 1963; Cooray 1997; Borovsky 1998; Marshall and Stolzenburg 2001; Maggio et al. 2009; Nag and Rakov 2010; Cooray 2014) and for how it relates to other kinematic and microphysical processes in thunderstorms as a function of flash rate and size (Wiens et al. 2005; Kuhlman et al. 2006; Deierling and Petersen 2008; Bruning and MacGorman 2013; Mecikalski et al. 2015; Schultz et al. 2015; Bruning and Thomas 2015).

The methods used to estimate the electrical energy discharged by lightning are made indirectly due to the difficulty in measuring it (Cooray 1997). Past studies have used various methods to estimate the energy discharged by lightning (Cooray 1997), the first of which utilizes estimates of the electrostatic charge transferred and potential difference of individual lightning flashes and the charge regions within which they traversed, respectively (Wilson 1920; Malan 1963; Marshall and Stolzenburg 2001; Boccippio 2002; Maggio et al. 2009; Nag and Rakov 2010). Additional methods consider the optical radiation emitted by lightning to derive an electrostatic and optical energy relationship from which it may be predicted (Conner 1967; Guo and Krider 1982), the acoustic energy of a lightning discharge using the theory of shock waves (Zhivlyuk and Mandel'shtam 1961), and the temporal evolution of a lightning channel's growth in relation to assumed waveforms of the measured current carried by a lightning channel during its evolution to estimate the energy discharged at different stages of its development (Cooray 1997; Borovsky 1998).

Many past studies have employed methods to estimate the energy discharged by lightning flashes by using electrostatic considerations given the availability of in situ electric field and field change measurements from which the charge transferred by lightning flashes and potential difference between charge regions may be derived or estimated (Malan 1963; Hill 1979; Cooray 1997; Marshall and Stolzenburg 2001; Boccippio 2002; Maggio et al. 2009; Dahl et al. 2011a; Bruning and MacGorman 2013). These methods first derive the electric potential from electric field measurements collected from balloonborne soundings carrying electric field meters, and consider only the vertical component of the electric field to define the vertical structure of the potential through the path in which the balloon ascends. The charge transferred by individual flashes is then estimated by using surface field change data and lightning mapping array (LMA) source locations (Maggio et al. 2009). The electrostatic energy is estimated by relating it to the charge and potential neutralized by individual flashes $W = q\Delta\phi$, where q is the charge transferred by a lightning flash and $\Delta\phi$ is the potential difference between charge regions within which they traverse. These methods have been employed to study the energy discharged by lightning flashes

---

to examine their contribution to a storm's energy budget by modeling a storm as an electrical generator whose contribution to the global electric circuit depends on its vertical extent and updraft speed which acts as the net charge transport velocity which supports electrification and charging (Vonnegut 1963; Lhermitte and Krehbiel 1979; Williams and Lhermitte 1983; Williams 1985; Weinheimer and Few 1987), and may be used to predict lightning flash rates (Boccippio 2002; Dahl et al. 2011a,b).

A study by Boccippio (2002) further demonstrated the importance of accounting for the geometry of a thunderstorm. In addition to the depth and vertical velocities that were measured, consideration of a thunderstorm's width better allowed for retrieval of electrostatic quantities such as generator current, the electric field, and charge when no measurements of these quantities are available. Boccippio (2002) and Dahl et al. (2011a,b) used a parallel-plate model from which the electric field and power of a thunderstorm were related to its kinematics and geometrical properties to predict flash rate and may also be used to make estimates of the electrical energy of storms.

A substantial gap, however, remains in modeling storm total and individual flash electrical energy in relation to storm-scale kinematic and microphysical processes. At the global scale, whole-storm generator models, such as those in Boccippio (2002) and Dahl et al. (2011a,b), parameterized the thunderstorm's electrical structure as a set of parallel plates from which some fraction η of the total storm charge was discharged per flash. In this way, any storm can be characterized in terms of its contribution to the global electrical circuit and to trace gas chemistry budgets needed for global climate models. The models used to characterize the energy dissipated by individual lightning flashes (Cooray 1997; Borovsky 1998; Marshall and Stolzenburg 2001; Nag and Rakov 2010) were employed without reference to the net energy budget across a population of flashes as they focus entirely on the physical evolution of single lightning leaders alone and, therefore, do not have relevant application in attempting to relate the energy discharged by lightning to changes in a storm's meteorology (e.g., updraft speed and volume). Therefore, the purpose of this study is to adapt the parallel-plate model to a time-evolving sequence of individual discharges with variable width, intermingled within a shared storm volume for application with observed lightning datasets to characterize flash discharge energy throughout its lifetime for comparisons to a storm's kinematic and microphysics.

Previous works have made an effort to estimate the electrostatic charge and potential associated with lightning continuously through a storm's lifetime by making use of a capacitor model to predict lightning flash rates by defining the electrical charge structure of a thunderstorm as a dipole (Boccippio 2002; Dahl et al. 2011a,b). However, a capacitor dipole depiction of a storm as a whole (Fig. 1b) is inconsistent with complex charge structures that have been found to vary throughout the convective-to-anvil regions in observed and simulated thunderstorms (e.g., Fig. 1a; and in Stolzenburg et al. 1998; Brothers et al. 2018). An oversimplified depiction of a storm's entire charge structure does not capture the variability of charge organization in a complex charge structure, nor does it account for which charge regions the initiation and propagation

of lightning flashes occurred between. Bruning and MacGorman (2013) and Bruning and Thomas (2015) made an initial attempt at estimating flash energy using a simple parallel-plate capacitor discharge model for individual flashes that depended on the distribution of horizontal flash areas in thunderstorms observed with an LMA. In doing so, they recognized that all flashes are not of the same size, and that the mean flash size (defined as the square root of the area of the plan projection of the flash) shifts throughout a thunderstorm's lifetime. However, they did not quantify the electrical energy in proper physical units, and this study aims to correct that deficiency. Moreover, each lightning flash only taps into a fraction of the total available electrical energy of a storm. As flashes of varying sizes occupy a wide range of a storm's total volume, it is of interest to understand how well the parallel-plate discharge models, developed in terms of whole-storm energy budgets, adapt to a real distribution of lightning flashes that fluctuate in size with time (Fig. 1c).

Therefore, this study adapts the capacitor model of Bruning and MacGorman (2013) from which the energy discharged by individual flashes can be estimated by using their geometry to mimic the local charge configuration (i.e., positive and negative charge layers into which flashes tap) instead of that of an entire storm (Fig. 1c), similar to a recent virtual capacitor model defined by Koshak (2021). The size of the charge regions used to define the capacitor plates is represented by the spatial extent over which each flash propagates, thus preserving the idea that flashes are initiated between charge regions of various sizes (Bruning and MacGorman 2013). An idealized, per-flash capacitor energy discharge model is employed using simulated lightning flashes produced in the Collaborative Model for Multiscale Atmospheric Simulation (COMMAS; Wicker and Wilhelmson 1995; Mansell et al. 2010) to determine its usefulness in estimating the energy neutralized by individual flashes for observational lightning datasets. By estimating the electrical energy discharged by individual lightning flashes as a function of their physical dimensions (Bruning and MacGorman 2013) and breakdown electric fields estimated at the altitudes of their initiations (Boccippio 2002), and comparing them to those computed in COMMAS, the capacitor model can be adjusted to allow for more accurate flash discharge energy estimates in reference to a full electrostatic model for practical application to real lightning data. Given that a capacitor models the preflash energy which is not completely discharged by a flash as it is defined by the breakdown electric field leading up to their initiation, capacitor adjustment factors μ_c of the simulated flashes are retrieved by comparing COMMAS and capacitor estimates to consider the fraction of the capacitor model's energy that is neutralized by the median flash. We acknowledge that the method by which COMMAS simulates lightning flashes has many simplifications and cannot represent many details of natural flashes (e.g., constant conductivity is assumed along each channel). Nevertheless, it can generate reasonable 3D structures of charge in storms (Mansell et al. 2005, 2010; Calhoun et al. 2013; Fierro and Mansell 2017; Brothers et al. 2018). For similar-sized flashes, the energy dissipation reported for the simulated flashes in Mansell et al. (2010) match quite well with the observation-based flash energies in Maggio et al. (2009). It thus seems reasonable to use simulated flashes in the present study.
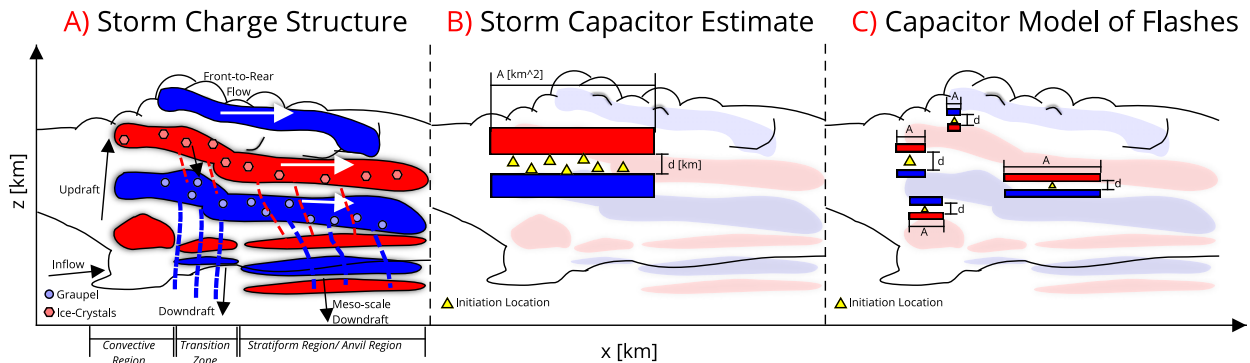
FIG. 1. Illustrations of a storm's charge structure as depicted by (a) Stolzenburg et al. (1998), (b) a parallel-plate capacitor model used to predict flash rates, power, and electrical energy of an entire storm (Boccippio 2002; Dahl et al. 2011a,b), and (c) a capacitor model adapted to fit the geometry of individual lightning flashes, which mimics the regions of charge and electric fields near locations of individual flash initiations. Terms A and d are the plate areas and separations, respectively, the red and blue color fills denote positive and negative charge, and red and blue dashed lines signify the fall streaks of hydrometeors. In (c) we note that this only illustrates where flashes may initiate in a storm in relation to their size, and do not mean it to show the simultaneous initiation of four flashes, nor does it depict the environments within which we employed the capacitor model.

The capacitor model greatly simplifies the lightning discharge, and thus it is not clear how well it matches flash electrostatic behavior and energy change as modeled by the discharge in COMMAS. If the capacitor model proves reliable, and a suitable representative adjustment factor can be determined, it may be applied to quantify individual and ensemble flash discharge energies, as observed in thunderstorms by instruments that map the spatial extent of discharges [e.g., LMAs, the Huntsville Alabama Marx Meter Array (HAMMA) (Bitzer et al. 2013; Zhu et al. 2020), the Japanese Low Frequency (LF) Mapper (Wu et al. 2018)] by considering only their physical dimensions and estimated breakdown electric fields at their initiation altitudes.

2. Methods

a. COMMAS simulated flash data

Flash data were generated for two simulated storms using COMMAS. Configuration for these simulations are described in detail in Brothers et al. (2018). Electrification processes include inductive graupel–droplet and noninductive graupel–ice collisional charge separation, and small ion interactions (Mansell et al. 2005). A stochastic branched lightning scheme then allows for the fractal development of leader channels and resulting charge rearrangement in the simulated storm (Mansell et al. 2002). Channel propagation is determined by the electric field at the channel leader tip (Mansell et al. 2002). Since charge is predicted on the model grid, the charge can be rearranged at the scale of the resolved eddies, eddies at and less than the outer length scale of the inertial subrange (Bryan et al. 2003).

Because the kinematic characteristics of a thunderstorm are hypothesized to influence the initiation and distribution of flashes of various sizes, two cases were selected to ensure some variability in flash characteristics. The first case (herein WK82) was initialized with an idealized atmospheric sounding of a supercell thunderstorm (Weisman and Klemp 1982) with a mixed layer convective available potential energy (CAPE) of 3132 J kg^{-1} and a 0–6-km shear of 36 m s^{-1}. This simulation produced a total of 6905 flashes in approximately 50 min of model time. The second case (herein SL16) was modeled using a mobile balloon sounding launched on 22 May 2016 for a right-moving supercell thunderstorm that occurred over Slaton, Texas, in an environment with a mixed layer CAPE of 5237 J kg^{-1} and a 0–6-km shear of 23 m s^{-1}, with a more linear hodograph. This simulation had 5404 flashes in 140 min, where a subset of 2878 flashes were used from the right moving cell that was considered for this analysis. The right-moving cell maintained strong updraft speeds and continued to produce lightning until the simulation ended.

For each case, only intracloud (IC) flashes were used because their bimodal structure is assumed to match the geometry and discharge of the capacitor plates, and to remain consistent with the same types of flashes mapped by LMAs for which this model's intended use is for. Therefore, CG flashes were not considered. We recognize that real IC flashes sometimes traverse through more than two charge layers (Maggio et al. 2009); however, such complexity is difficult to handle with a simple model. Rather, we reason that because the capacitor model is used only to estimate individual flash discharge energies, then consideration of more complex charge structures is not required as their contribution to the electrostatic energy is already accounted for by the breakdown electric fields used to estimate them. The IC flashes represented a total of 99.67% and 98.43% of the entire WK82 and SL16 flash populations, respectively. The gridpoint channel data for each simulated IC flash were saved as a set of nodes and connections, permitting reconstruction of the branched channel tree. A Delaunay triangulation was used to calculate the plan-view convex hull of each flash (Bruning and MacGorman 2013). The area of the convex hull was used as the area A in the capacitor model for each flash. The two largest local maxima in the bimodal vertical distributions of channel segments were used to

define the position of the capacitor plates and their separation d, and the altitude of initiation was used to predict the electric field at initiation via the runaway breakeven electric field threshold (Dwyer 2003).

The electrical energy discharged by individual flashes is defined in COMMAS as a difference between the post and preflash storm electrical energy which defines how much energy was neutralized by a flash. The storm electrical energy at either pre- or postflash state is defined by a discrete sum of the product of the charge density and potential at each grid point in the model domain,

$$W_m = \frac{1}{2}\left[\sum_i^N \rho(x_i)\phi(x_i)\Delta V\right], \tag{1}$$

where the subscript m signifies the model domain energy, $\rho(x_i)$ and $\phi(x_i)$ are the net charge density and electric potential at each grid point x_i in the model domain with a total of N grid points, and ΔV is the volume of each grid point. The flash discharge energy is then computed as

$$\Delta W_m = W_{m,\text{post}} - W_{m,\text{pre}}. \tag{2}$$

The energy discharged by the simulated lightning flashes from Eq. (2) is assumed as "truth" for this study as it considers the change in energy that is derived from time-evolving 3D complex charge structures that are coupled to a storm's kinematics and microphysics which give a better representation of flash discharge energy than by using simple 1D models. However, that these values are physically representative of actual discharge energies in nature cannot be concluded since COMMAS itself makes assumptions for the propagation of individual lightning channels (e.g., constant high conductivity of all channels; Mansell et al. 2005).

b. Electrostatic energy neutralization by lightning flashes

1) CAPACITOR DISCHARGE MODEL

The electrical energy stored by an ideal parallel-plate capacitor is well known, and assumes that the plate spacing is much less than the span of the plate area, approximating infinite sheet geometry. The formula for the energy stored by a capacitor is generally written as

$$W_c = \frac{Q^2}{2C}, \tag{3}$$

where the subscript c signifies the capacitor model, Q is the total charge, $C = \epsilon A/d$ is the capacitance, and ϵ is the electric permittivity of air ($\epsilon = 8.858 \times 10^{-12}\,\text{CV}^{-1}\,\text{m}^{-1}$), A is the plate area, and d is their separation. Equation (3) can also be written in terms of the electric field between the capacitor plates,

$$W_c = \frac{\epsilon}{2}|E|^2 V, \tag{4}$$

where E is the electric field between the plates, and $V = Ad$ is the volume between them. The homogeneous electric field between the plates is that for infinite sheet geometry,

$$E = \frac{\sigma}{\epsilon}, \tag{5}$$

where σ is the surface charge density of the plates. The electric field for infinite sheet geometry was assumed as a parallel-plate capacitor discharge model requires that the effect of plate area is much greater than their separation. However, in the case that the plate width, or square root of its area, is smaller than its separation, then this assumption would be violated and the capacitor model would give estimates that are comparable to a point-charge model. We made use of the finite disk model of Boccippio (2002) to test the sensitivity in estimating the energy discharged for various plate sizes as defined by the lightning flashes analyzed in this study as it relaxes from infinite-sheet to point-charge geometry. In doing so, we determined that a capacitor model's geometry, as defined by individual flashes, impacts our estimates only for the smallest flashes (≤ 1 km in width), and so we do not consider it for this study as differences between models were small ($<7\%$). Rewriting Eq. (4) in terms of the surface charge density and capacitor dimensions results in

$$W_c = \frac{\sigma^2 Ad}{2\epsilon}. \tag{6}$$

In this study, Eq. (6) is used to model the energy discharged by individual flashes by assuming the horizontal areas and separation of bidirectional leaders as the plate areas A and separation d of the capacitor model, respectively. Furthermore, by defining the capacitor areas by the horizontal channel structures of each flash, then both positive and negative components of each flash are assumed to be of equal size so as to maintain a parallel-plate depiction.

We define Eq. (6) as an idealized capacitor model that is only used to estimate the energy discharged by lightning flashes by considering the electric fields estimated at their initiation locations and their geometries. The capacitor model is independent of the storm environment within which flashes were initiated, and so we need not consider external charge contributions, the charge induced on Earth's surface, and image charges as these affects are captured by the breakdown electric fields and electrical energy.

Equation (6) is similar in appearance to, but physically different from, the model proposed in Bruning and MacGorman's (2013) Eq. (31), which defined the energy stored by a capacitor in terms of a space charge density by relating the total charge of a capacitor [Eq. (3)] to a charge flux carried by vertical motion, such that $Q = IT = JAT$, where I is the charging current between the plates, J is the charge flux, A is the area, and T is the flash time interval. Furthermore, the flash time interval was equated to the convective velocity w of a storm by $w = d/T$ which describes the change in distance of the charge flux with time, and the charge flux J was defined further by $J = w\rho = \rho d/T$, where ρ is the space charge density between the plates. The relation between the total charge Q to the charge flux J carried by some convective velocity w, when used in Eq. (3), results in the formulation of the capacitor discharge model as

$$W_{\text{BM}} = \frac{\rho^2 Ad^3}{2\epsilon}, \tag{7}$$

where the subscript "BM" denotes the model of Bruning and MacGorman (2013). Their version of the capacitor model

assumes a charging current defined by some convective velocity that transports a constant charge flux through a fixed storm depth, where the energy neutralized by a flash is a function of only the areas of individual flashes. We can compare the capacitor model in Eq. (6) to that of Bruning and MacGorman (2013) in Eq. (7) to identify their differences by assuming that $\sigma = Q/A$, and $Q = \rho V = \rho A d$, thereby assuming a charge flux exists by considering a space charge density ρ,

$$W_c = \frac{\rho^2 A d^3}{2\epsilon} = W_{BM}. \tag{8}$$

The difference of the model used in this study to that of Bruning and MacGorman (2013) is the use of separation d values that vary and no longer depict a fixed charge region separation of a storm, but rather the local charge separation for individual flashes, and so the definition of a charging current is not needed.

Equation (6) frames the total electrostatic energy of lightning flashes as a function of their size and mimics the physical separation of the positive and negative charge regions in which they develop. In addition, the charge of each plate is assumed to be equal and opposite, but the sign orientation is irrelevant because E and σ are squared terms in the capacitor model [Eqs. (4) and (6)], and E is assumed to be generated by both plates without needing to account for their polarities. Moreover, Eq. (6) requires knowledge of σ to make estimates of the electrical energy. Because measurements of charge are not usually available, a method to retrieve unique values of σ is discussed in the following section.

2) CHARGE DENSITY RETRIEVAL

Boccippio (2002) introduced a method by which a charge density upon the initiation of a lightning flash may be estimated from the pressure-dependent runaway breakeven electric field threshold at the altitude of initiation (i.e., scaled by atmospheric air density with height; MacGorman et al. 2001; Dwyer 2003; Marshall et al. 2005),

$$E_{init} = E_{th} e^{-z_{init}/8.4}, \tag{9}$$

where z_{init} is the initiation altitude of a flash in km, and $E_{th} = 281 \, kV \, m^{-1}$ is the runaway breakeven threshold at sea level (Marshall et al. 2005). It should be noted that while Eq. (9) fits the observed maximum electric field profiles (Marshall et al. 2005), and accounts for the initiation altitude, we do not mean to suggest it is the mechanism by which breakdown occurs. Rather, we use it as a matter of convenience and to be consistent with the method by which COMMAS determines the electric field criteria to initiate lightning (Mansell et al. 2002). In this study we assume that all lightning flashes initiate halfway between the capacitor plates.

While the critical surface charge density for breakdown is not needed for the energy calculation, it is given by

$$\sigma_{critical} = \epsilon E_{init}. \tag{10}$$

3) MODEL ENERGY ADJUSTMENT FACTOR

A capacitor model describes the total energy for a given initiation electric field and an implied critical surface charge

density, with all charge needed to produce E_{init} consolidated on the capacitor plates prior to initiation. This is because W_c is a function of E_{init} and flash geometry, and so it predicts the total energy of a capacitor for electric field values that were required to initiate a flash. Contrast the localized charge implied by the capacitor with the entire storm energy W_m, which is computed by taking the sum of the product of the electric potential and charge density at each grid point in the simulation domain (Fig. 2a). The capacitor model acts as the only source of charge at electrical breakdown, and it is expected to overestimate the energy because of two assumptions: that the electric field has the breakdown value uniformly within the flash volume, and that a flash completely dissipates all the energy. Thus, an adjustment is required such that it may be applied for estimating flash energy in reference to a full 3D electrostatic model.

Initiation of lightning flashes in COMMAS only requires E_{init} be realized within a single grid cell whose volume depends on the selected grid spacing of a simulation (for this study, the grid cell volumes were of size $125^3 \, m^3$; Fig. 2b). However, for the capacitor model, $\sigma_{critical}$ and E_{init} are distributed across the plates and whole volume between them which is defined by the variable geometry of each flash (Fig. 2c), and so each capacitor is assumed to contain a large constant electric field rather than one that varies in a storm with a more complex charge structure. Therefore, W_c overestimates the local preflash energy by a factor related to the ratio of the volume between capacitor plates and that of the actual volume in the simulations in which E_{init} exists. The second unknown factor is the fraction of local energy actually dissipated by the lightning flash. For this reason, it is necessary to introduce a universal adjustment factor that can account for both unknown factors in the flash energy.

The model adjustment factor of the capacitor model is given by the ratio of energy dissipated by the model flash energy to the capacitor model energy,

$$\mu_c = \frac{\Delta W_m}{W_c}, \tag{11}$$

and although it mathematically resembles the neutralization efficiencies η introduced in Boccippio (2002) and Dahl et al. (2011a), it is conceptually different and does not hold the same significance. The ratio μ_c compares the actual simulated flash energy with those estimated by the capacitor and will vary from flash to flash. However, a unique μ_c cannot be determined for observed lightning flashes since it is related to the unknown distribution of charge in real storms. For the eventual purpose of applying these equations to observational data, we aim to identify a statistical representative $\tilde{\mu}_c$ defined by the median of all μ_c to both approximate a universal adjustment factor to compute the capacitor flash discharge energy W_d,

$$W_d = \tilde{\mu}_c W_c. \tag{12}$$

The median of μ_c was chosen instead of the mean to avoid bias due to outliers, and because the distribution of all μ_c values was lognormal and so the mean does not depict the most probable value (Fig. 3). However, it should be noted that differences between the mean and median μ_c for the two cases presented in this study were small (0.0014 and 0.004 for WK82 and SL16,
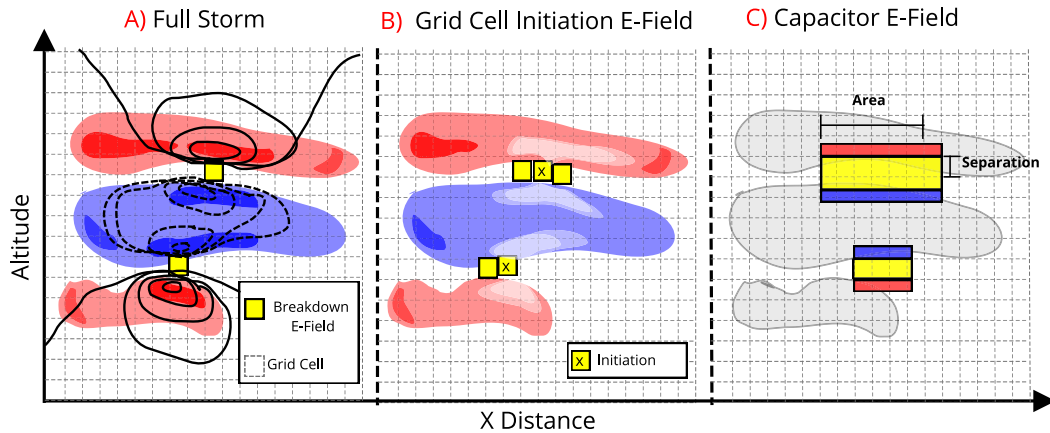
FIG. 2. Illustrations of how (a) W_m is computed by considering a storm's electric potential structure (solid and dashed lines) and charge densities (color fill) at each grid cell within a simulation domain, (b) $W_m(E_{init})$ is computed at the exact location of a flash initiation which is restricted to a single grid cell, and (c) $W_c(E_{init}, d, A)$ is computed using the capacitor model. Yellow squares signify where the electric field achieved a breakdown value, red and blue color fields in (a) and (b) depict the charge densities ρ and solid and dashed lines in (a) depict the large-scale potential ϕ structure at each grid cell x_i of size 125^3 m^3 where white shaded regions depict the depleted charge upon flash initiation and termination, red and blue color fields in (c) depict the capacitor plates defined by lightning flashes used to mimic the local charge structure near their initiations.

respectively) but not exactly the same, and so we make use of the median for the eventual purpose of using this model for observed datasets, as it will always depict the value representative of most flashes where the mean will not.

For reference, the fraction of the simulation domain energy discharged by each flash in COMMAS is given by

$$\eta_m = \frac{\Delta W_m}{W_m}, \quad (13)$$

where its median is written as $\tilde{\eta}_m$. Note that μ_c and η_m represent distinct physical values: η_m is the fraction of a storm's total energy removed by each flash, whereas μ_c is a scaling adjustment for just the local energy within the flash volume. Here, η_m is used only to illustrate how accounting for the entire storm electrostatic energy differs from a ore simpler flash-centric capacitor model, especially for the cases at hand where the storms grow substantially larger than the typical thunderstorm cell.

c. Summary of research questions

The COMMAS simulations provide a reference to compare the capacitor energy estimates, allowing us to investigate the appropriateness of the capacitor model for predicting the electrical energy of lightning flashes observed using LMAs. We will address the following predictions that follow from the concerns outlined in the introduction.

The first question is whether application of the capacitor model can accurately reproduce the flash energy trends, demonstrating its fitness of purpose for observational estimates of flash energy. Then a second question is whether the additional detail required by the capacitor model (i.e., flash geometry) is worth the additional effort compared to a simpler scaling methods that accounts for flash rate but not individual

flash areas—i.e., each flash discharges the same amount of electrostatic energy (Boccippio 2002; Dahl et al. 2011a).

In the present study, the dipole structure of the flash capacitor model is assumed to only mimic the local charge regions of opposite charge that generated the electric field E_{init} to initiate a lighting flash, rather than depicting the whole storm's charge structure. Therefore, we expect μ_c to be systematically different from η_m since the capacitor energy is characterized by
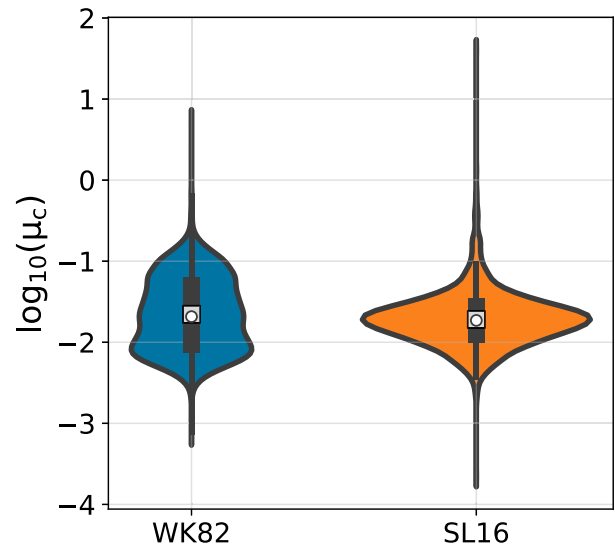

FIG. 3. Violin plots of the distributions of μ_c for WK82 (blue) and SL16 (orange). The white circles and squares depict the median and mean μ_c, respectively, and the gray rectangles within each violin plot depicts the interquartile range of the distributions for reference.
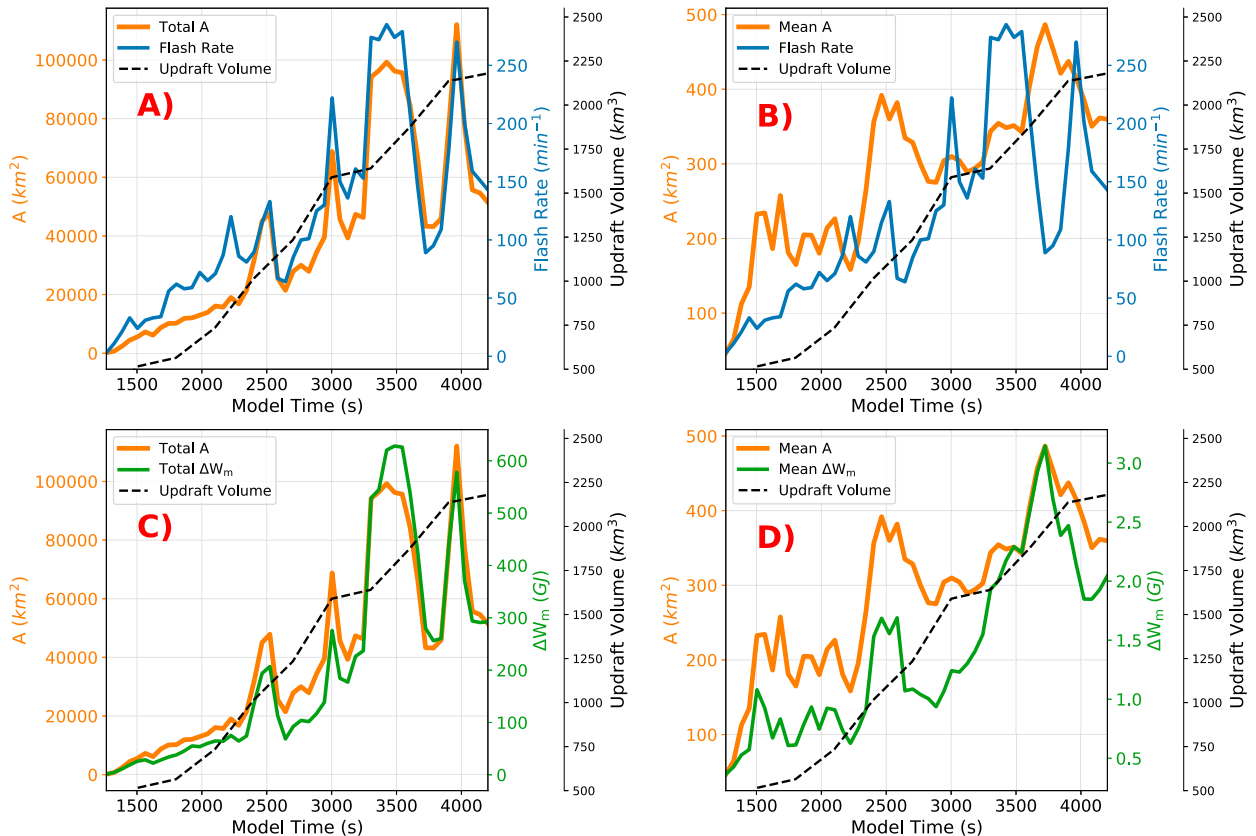
FIG. 4. Each panel illustrates the time series of updraft volume, for updraft velocities greater than $10\,\mathrm{m\,s^{-1}}$ (dashed), against (a) total flash rate (blue) and total flash areas (orange), (b) total flash rate (blue) and mean flash area (orange), (c) total flash energy (green) and total flash area (orange), and (d) mean flash energy (green) and mean flash area (orange), in 1-min intervals throughout the model simulation for WK82.

both E_{init} and flash area which varies for each flash. The value of W_c will also vary with each flash's initiation altitude since E_{init} is pressure dependent.

3. Results—Flash activity

Temporal analyses were made to examine how the simulated flash rates, areas, and electrical energy neutralized ΔW_m evolved in time for each simulated storm in comparison to the volume of the updraft in excess of $10\,\mathrm{m\,s^{-1}}$. In addition, these analyses provide insight as to how the simulated lightning activity compares with what is generally observed in real storms (Wiens et al. 2005).

a. Case 1—Weisman and Klemp (1982)

Figure 4 summarizes the simulated flash rates, areas, and electrostatic energy change ΔW_m for 1 min intervals. Also shown at 5-min intervals is the volume of updraft velocity $> 10\,\mathrm{m\,s^{-1}}$. Figures 4a and 4c show that the totals of flash area and electrostatic energy closely follow flash rate and generally correlate to a steady increasing updraft volume. The simultaneous increases in updraft volume and flash rate throughout the simulation indicated a strengthening convective core and charging processes (e.g., Wiens et al. 2005; Deierling and Petersen 2008).

Figures 4b and 4d further detail the average behavior of these flash characteristics relative to the total flash rates and updraft volume. Figure 4b shows that local minima in flash area tend to be associated with local maxima in rate (Bruning and Thomas 2015), although both generally increase as the storm grows.

The largest fluctuations of the mean flash area and energy were at times when the flash rates were the highest, at 2500, 3000, 3250, and 4000 s. Prominent increases in mean flash area tended to occur with lower flash rates and higher mean flash energy, particularly at 2500 and 3750 s. The evolution of the mean flash energy closely followed the mean flash area (Fig. 4d), indicative of larger areas implying larger energy.

These trends demonstrated that changes in the mean flash energy were dependent on the variation of flash sizes, defined by a Pearson correlation coefficient $r = 0.91$ (Fig. 5a), and were also correlated to the updraft volume, with a Pearson $r = 0.85$ (Fig. 5e). Furthermore, the correlation, as a function of time, of total flash energy with total flash area is better than flash area with flash rate (Fig. 5c).

b. Case 2—Slaton, 22 May 2016

Figure 6 summarizes the simulated flash rate, area, and energy change ΔW_m characteristics for the right-moving supercell
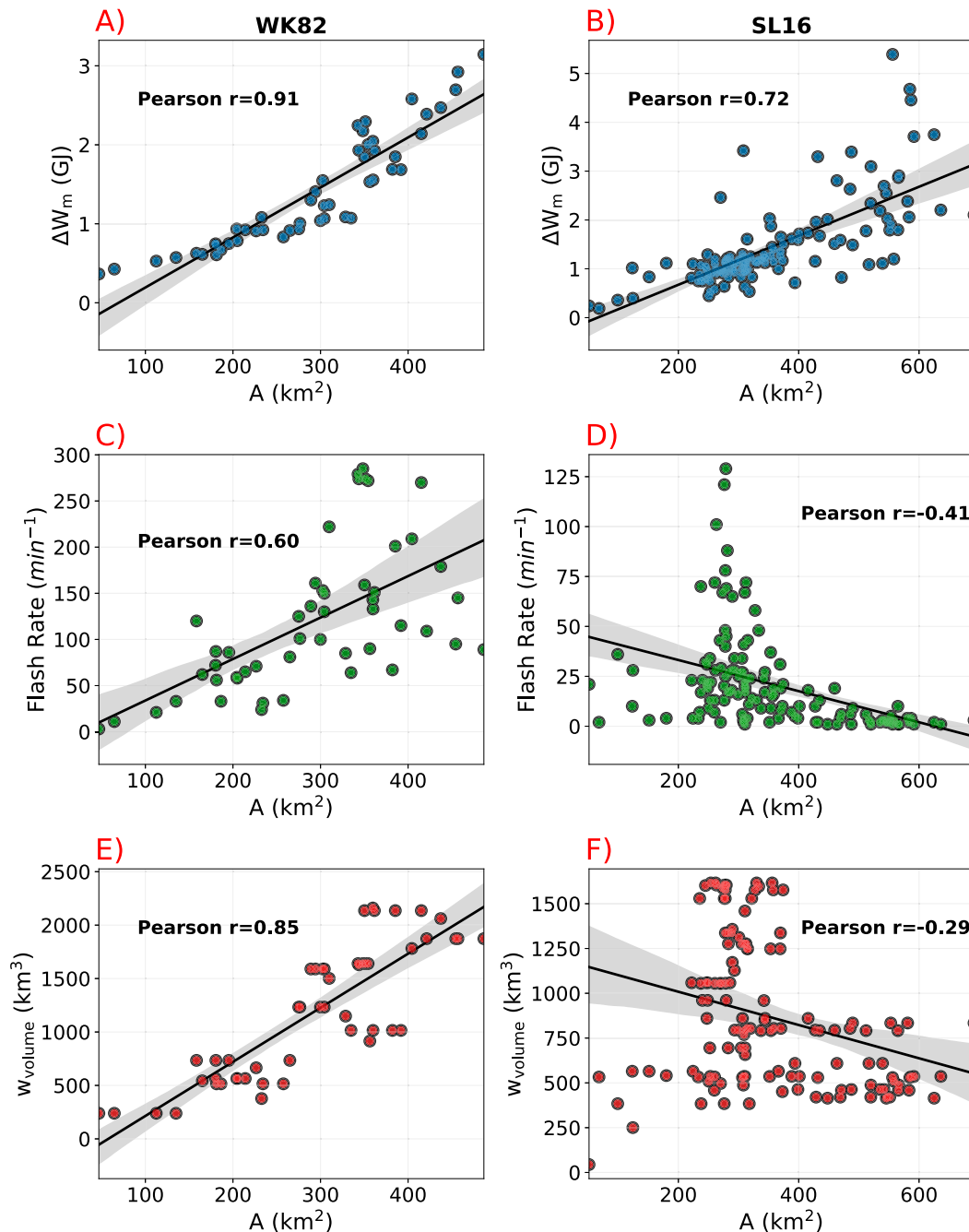
Fig. 5. Linear regressions for 1-min-averaged (a) W_m, (c) flash rate, and (e) updraft volume for WK82, and (b) W_m, (d) flash rate, and (f) updraft volume for SL16 in relation to flash area. Pearson r values are annotated in each panel, black line is the linear fit, and gray shaded regions are the regression confidence interval.

storm, SL16. As seen for WK82, from Figs. 6a and 6c, the totals of flash areas and energy closely aligned with flash rates throughout the simulation time. Additionally, the temporal evolution of flash rate followed that of the updraft volume, as found for WK82.

From Figs. 6b and 6d, the mean flash characteristics demonstrated that the mean flash areas were highest prior to the intensification of the storm, as indicated by small updraft volumes

and low flash rates, and decreased with increasing flash rates and updraft volume. Mean flash energy also tended to align with the variations in flash size, such that the occurrence of larger, less frequent flashes in the first half of the simulation coincided with the largest mean flash energy, and the smaller flashes in the second half coincided with less flash energy.

As with WK82, the mean flash energy and flash area covaried closely as determined by a Pearson correlation coefficient of
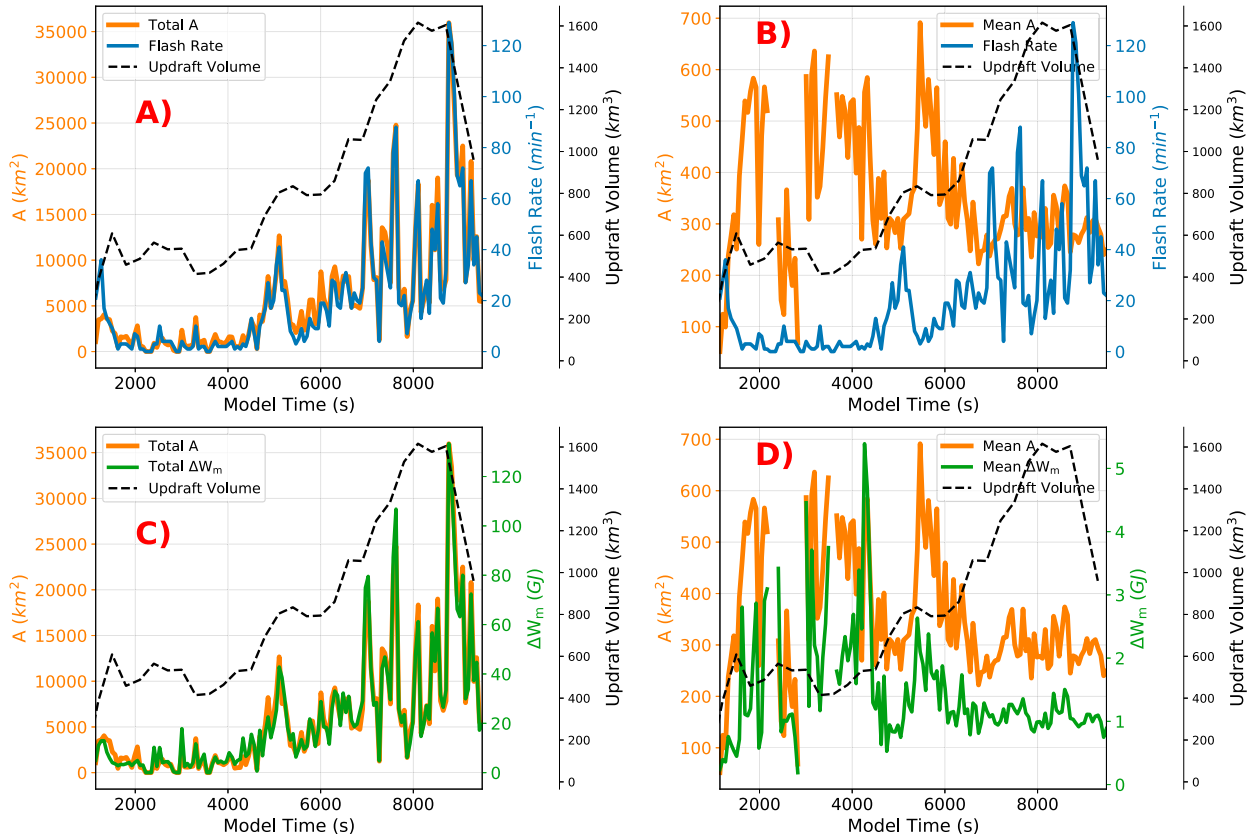
FIG. 6. As in Fig. 4, but for SL16. Each panel illustrates the time series of maximum updraft intensity (dashed) against (a) total flash rate (blue) and total flash areas (orange), (b) total flash rate (blue) and mean flash area (orange), (c) total flash energy (green) and total flash area (orange), and (d) mean flash energy (green) and mean flash area (orange), in 1-min intervals throughout the model simulation for SL16.

$r = 0.72$ (Fig. 5b), in contrast to poor correlations to flash rate and updraft volume, defined by $r = -0.41$ and -0.29, respectively (Figs. 5d,f). The relation of flash area to flash rate and updraft volume were poorly defined and showed that flashes with areas between 200 and $400\,\mathrm{km^2}$ were frequently initiated when the updraft was largest in size. When the updraft volume was small, the flash areas were either <200 or $>400\,\mathrm{km^2}$, and so no correlation was found.

4. Results—Capacitor model estimates and adjustments

One minute total and mean capacitor W_c and model ΔW_m flash energy trends varied similarly in time (Fig. 7). However, W_c was between 20 and 160 times larger than ΔW_m, and so capacitor adjustment factors $\tilde{\mu}_c$ were computed to find the fraction of the capacitor energy to represent the flash energy.

The median capacitor adjustment factors were $\tilde{\mu}_c = 0.021$ and 0.019 for WK82 and SL16, respectively. The median values for the domain energy discharge fraction $\tilde{\eta}_m$ were larger, falling between 0.06 and 0.03 for WK82 and SL16, respectively. Although $\tilde{\eta}_m$ and $\tilde{\mu}_c$ are fundamentally different, a factor difference ranging from 2 to 3 was found between them, indicating that W_c is generally even larger than the simulated total storm electrical energy. The difference between $\tilde{\eta}_m$ and $\tilde{\mu}_c$ can be attributed to how W_c

overestimated the total energy for most flashes given that it is largely dependent on flash area, as illustrated in Fig. 2c. Thus, a flash area influence on how the adjustment factor μ_c of individual flashes are determined for W_c was examined.

We first check for any systematic flash area dependence for μ_c populations prior to adjusting W_c. Figures 8a and 8b illustrate the distribution of μ_c, and for reference η_m, for both cases as a function of flash area, and is log scaled because μ_c and η_m spanned several orders of magnitude at smaller flash sizes. More than 99% of flashes had widths greater than 1 km, with about 97% of the flashes being larger than 10 km in width.

A handful of instances of $\mu_c > 1$ at length scales less than $3.16\,\mathrm{km}$ indicated the capacitor model rarely underestimated the COMMAS flash energy for the smallest flashes ($<1.5\%$ of either flash population). Because $>97\%$ of all flashes were greater than 10 km in width, however, the capacitor model largely overestimated the discharge energy, and so $\tilde{\mu}_c$ was much smaller than 1 (on the order of 10^{-2} to 10^{-3}) for larger flashes. We speculate that an apparent dependance on flash size for μ_c is a result of the capacitor energy W_c considering only a single value of the electric field at breakdown to compute a preflash W_c, and is scaled by the flash area which results in predicted values with a difference of up to two orders of magnitude larger than ΔW_m. Therefore, the fraction of capacitor energy neutralized by a flash
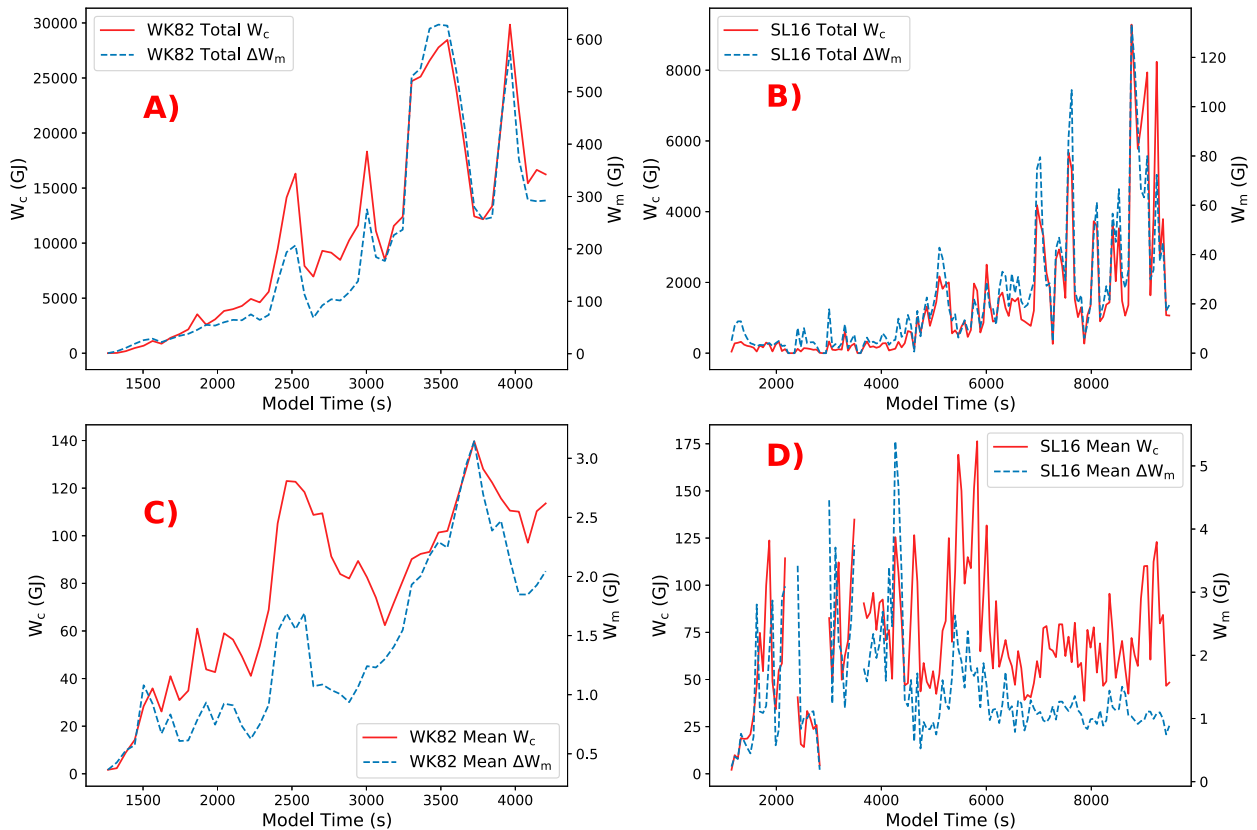
FIG. 7. Estimated capacitor electrostatic energy W_c (left axis) are compared to simulated energy ΔW_m (right axis; dashed blue): (a),(b) the total 1-min energy estimates and (c),(d) the 1-min mean flash energies.

should be lower to compensate for this overestimation due to an overrepresentation of E_{init} existing everywhere between the capacitor plates.

Figures 8c and 8d show ΔW_m as a function of flash size, and it exhibited a power-law scaling that was consistent with the 5/3 line shown for real flash energy estimates in Bruning and MacGorman (2013). Also shown is W_c, which exhibits a large overestimate for the large flashes that dominate the population, while the smaller flashes are closer to correctly scaled. After application of a constant $\tilde{\mu}_c$ to calculate W_d (not shown in Fig. 8), the energy in the large size bin is closer to correct, while the smaller flash energies are underestimated.

5. Results—Capacitor model adjustment

Application of $\tilde{\mu}_c$ to give a final flash energy estimate W_d from the capacitor model is shown in Fig. 9. The total flash energy trends for both WK82 and SL16 were found to follow COMMAS flash energy ΔW_m closely, though there are some departures that remained less than a factor of 2 different at any one time (Figs. 9a,b). The mean COMMAS and capacitor energies per flash also varied similarly in time (Figs. 9c,d). The largest differences were about a factor of 2 larger than capacitor mean flash energy in WK82 between 2200 and 3200 s, and a factor of about 3 larger than COMMAS mean flash energy before 5000 s in SL16.

The individual adjusted energy estimates were then compared to the model ΔW_m (Fig. 10). After adjustment, the distribution of the capacitor estimates were close to those of ΔW_m. For WK82 (Fig. 10a), most flashes discharged energy < 5 GJ in magnitude indicative of smaller more frequently initiated flashes discharging less energy later into the simulation duration. The distribution of ΔW_m, however, was constrained to magnitudes < 6 GJ, whereas those for W_d were >15 GJ. These overestimates reflect the geometric constraints by which the electric field E_{init} is forced to represent between the capacitor plates, and demonstrate why μ_c must be small to adjust energy estimate to match magnitudes of ΔW_m properly. Furthermore, this departure in energy magnitudes is also shown in Fig. 9c indicating that at simulation time 2500 s, larger flashes were initiated and were estimated to neutralize more energy than any other time. For SL16 (Fig. 10b), the distributions of both ΔW_m and W_d were in good agreement, and showed similar maximum and minimum energy values both from the individual energy estimates themselves and from the energy trends, with a drop in the number of flashes discharging the smallest energy values < 2 GJ in magnitude (Fig. 9d).

Variability in the estimates of W_d in comparison to ΔW_m identified from Fig. 9 and their energy distributions in Fig. 10, over the lifetime of each simulation, further demonstrated that the capacitor predicted energy trends were not exactly the same to those of COMMAS. To define how well the capacitor
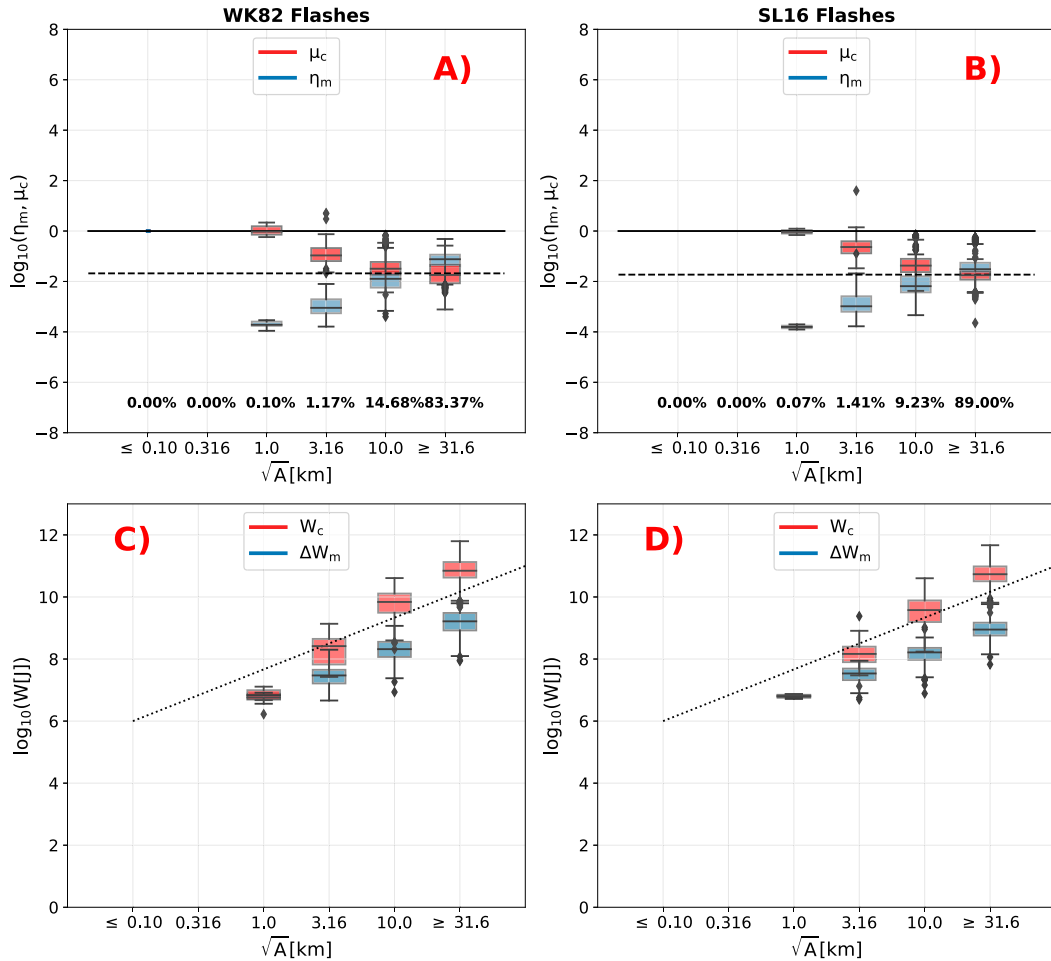
FIG. 8. (a),(b) Boxplots of log-scaled adjustment factors μ_c (capacitor) and model neutralization efficiencies η_m (COMMAS) where the horizontal dashed line is $\tilde{\mu}_c$, the solid horizontal line is a reference line to a magnitude of 10^0, and (c),(d) boxplots of log-scaled W_c and ΔW_m as a function of flash length $\sqrt{A}$, where the dotted line is the reference $-5/3$ slope. Flash lengths are not log scaled, but their magnitudes were binned in increments $\log_{10}(\sqrt{A}) = 0.5$. Outliers are shown by diamond markers, and percentages annotated in (a) and (b) represent the fraction of flashes associated with each flash length bin. Bin labels correspond to the right edge of each bin. Capacitor model adjustment factors and discharge energies are shown in red, and those of COMMAS are in blue.

discharge model W_d diagnosed the energy neutralized ΔW_m for each flash population, W_d and ΔW_m were totaled and their ratios calculated in 1-min intervals to examine by how much the capacitor model overestimated the flash discharge energy (Fig. 11). The capacitor discharge model was found to overestimate the duration total energy by 11.6% for WK82 and by 15.0% for SL16 for all flashes. Other than one extreme outlier for SL16, the ratios spanned 25% to 200%, and were more variable in the SL16 case reflecting the higher-frequency oscillations in the flash rate at the later stages of the storm's life cycle.

6. Discussion

a. Are estimates comparable to previous studies?

Adjusted capacitor estimates were expected to match the magnitudes of COMMAS solutions as they were assumed as

"truth." However, how well COMMAS computes flash energy solutions were compared with flash energy estimates from past work. For both cases, flashes neutralized and minimum and maximum of 10^6 to 10^{10} J of energy, spanning four orders of magnitude. Such spread in flash discharge energy has also been estimated using different methods in previous studies.

Estimates of flash energy using assumed, or derived, values of the charge transferred by lightning flashes and the potential difference between the charge regions within which they propagated have showed typical values ranging from 10^7 to 10^{10} J of energy (Cooray 1997; Borovsky 1998; Marshall and Stolzenburg 2001), which matches the range of ΔW_m in this study. In addition, a study estimating the energy discharged per unit length of lightning channels were found to be on average on the order of 10^4 J m^{-1} (Hill 1979), in range of similar estimates made for both the smallest (1 km) and
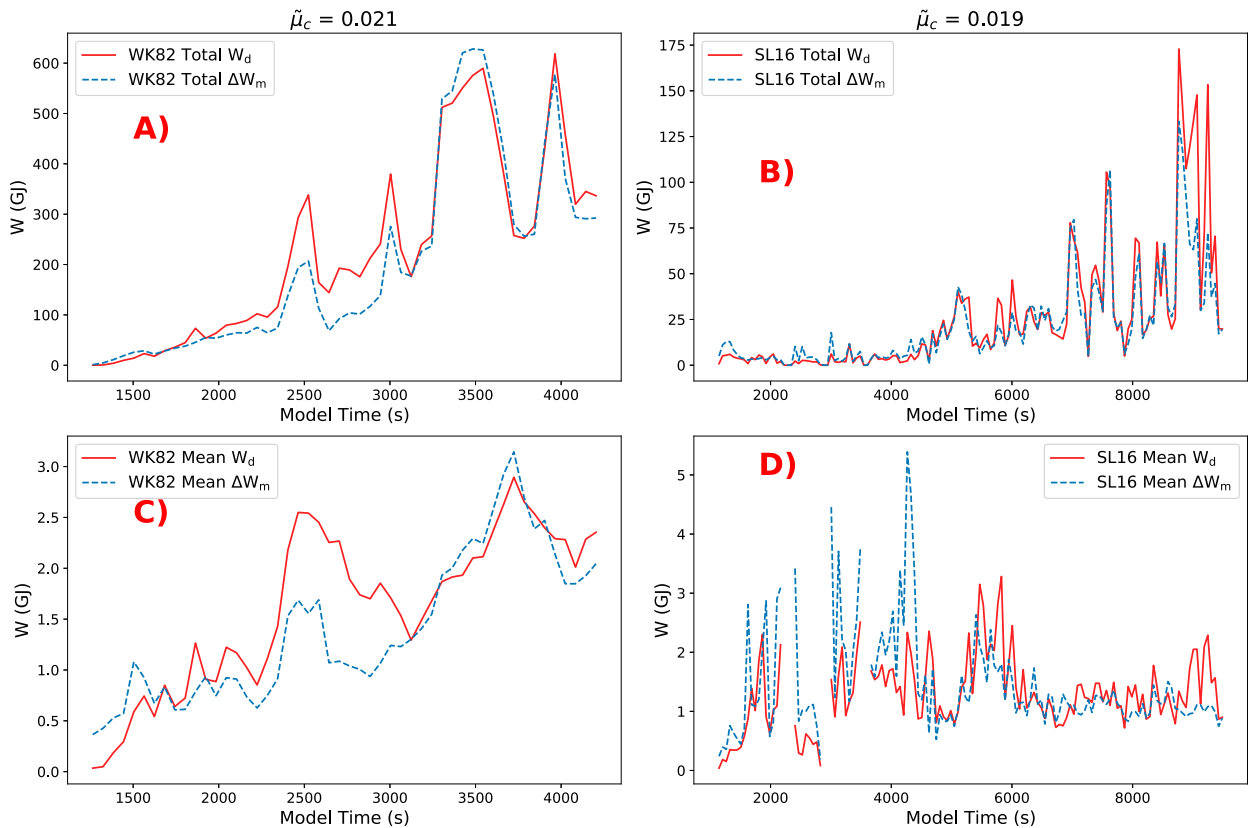
FIG. 9. Time series of adjusted (a),(b) total and (c),(d) mean flash energy for the capacitor model (W_d, red) compared to simulated flash energy (ΔW_m, blue dashed) using the median $\tilde{\eta}_c$ as indicated in the label at the top of each column. The columns show (a),(c) WK82 and (b),(d) SL16.

largest (>36 km) simulated flashes with energy values ranging from 0.1 to 28×10^4 J m^{-1}.

As shown in Fig. 10, flash energies were most frequently <1 GJ in magnitude, in range of estimates made by Maggio et al. (2009) (0.2–7 GJ) and Mansell et al. (2010) (0.2–0.8 GJ). Therefore, use of ΔW_m solutions as a reference energy by which to adjust our capacitor model remains a sound choice, and further exemplifies that simpler models that make use of

typical measured electrostatic values by which to estimate flash energies produce results that are comparable to a full 3D physics model. The adjusted capacitor estimates, however, spanned six orders of magnitude ranging from 10^4 to 10^{10} J of energy. The lower end of the capacitor estimates in this study (<10^6 J) can be attributed to our use of a single representative adjustment factor $\tilde{\mu}_c$ which introduced bias toward larger flashes, and thus leads to adjusting smaller flash energies to
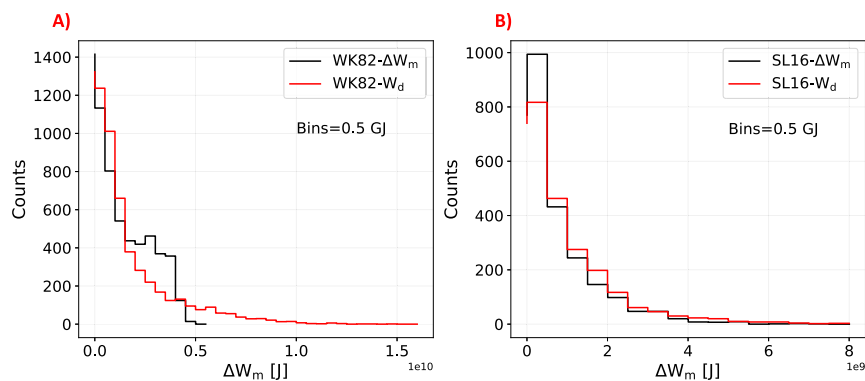

FIG. 10. Histograms of model ΔW_m (black) and capacitor-adjusted W_d (red) for (a) WK82 and (b) SL16. All discharge energy populations are binned in increments of 0.5 GJ.
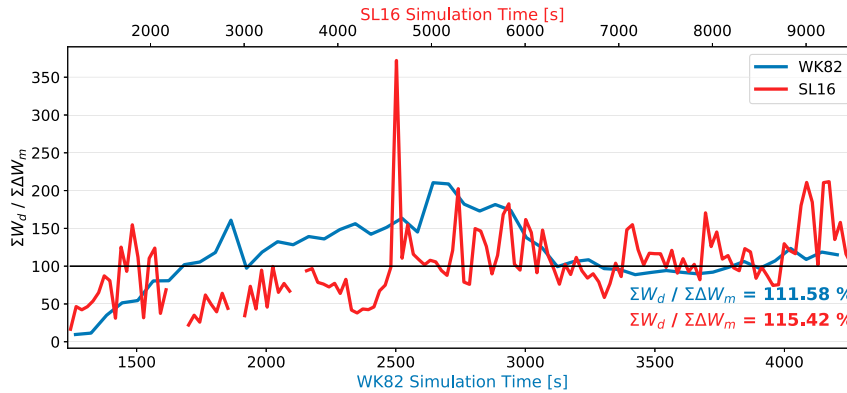
FIG. 11. Time series (each minute) of the total energy ratio $W_d/\Delta W_m$. The total energy ratios are annotated and colored for each simulation. Solid black line illustrates where the energy ratios are 100%.

much lower values. We discuss these errors in the following section.

b. μ_c, flash width, and errors

The simulations showed that η_m increased for flashes that filled more of the storm volume. As expected, these larger flashes tapped more of the available electrical energy.

The interpretation of the decrease in μ_c for larger flashes is more subtle. From Figs. 8a and 8b, μ_c is closest to 1 for the smallest flashes, where the capacitor model apparently comes closest to being an accurate model of predischarge configuration of localized charge that produces the electric field needed for initiation. This suggests that in small flashes, a relatively large fraction of the flash volume has electric field magnitudes close to the initiation threshold. μ_c decreases as flash sizes increase, and this suggests that the large field magnitudes are confined to decreasingly smaller fractions of the encompassing capacitor volume. For this reason, W_c is much larger than ΔW_m, and so μ_c is much smaller (two orders of magnitudes) than for smaller flash sizes.

The variability in the energy adjustment factor μ_c as a function of flash size (Fig. 8) is an indicator of the degree of error to be expected when choosing a single energy correction factor to be applied to a population of flashes of varying width. Overall, the errors are fairly symmetric about the median line, and so at first glance one might assume errors in either direction would average to zero. However, here the logarithmic visualization misleads. A simple calculation demonstrates that the errors grow much faster (exponentially) for scaling factors that are further away from 1. Assuming $\tilde{\mu}_c = 0.035$ and $W_c = 1\,\text{GJ}$, $W_d = 0.035\,\text{GJ}$. At a flash size scale of 5 km, the appropriate value of μ_c is about a factor of 10 larger, so the flash energy values should be $W_d^* = 0.35\,\text{GJ}$, or a -90% absolute error in W_d. If the μ_c were instead about a factor of 10 smaller ($\mu_c = 0.0035$), the energy estimate would be $W_d^* = 0.0035\,\text{GJ}$, or an absolute error of 900%.

Given the dependence of μ_c on flash area (Figs. 8a,b), we also tried to fit a linear regression to the log-scaled flash area, thereby avoiding the need to calculate a median μ_c. However, the performance of this method was worse. Errors unique to

each flash's predicted μ_c propagated into both the time trends analysis and energy distributions, and resulted in a departure in the shapes of the energy trends in relation to those of ΔW_m. Therefore, we did not consider it further.

c. μ_c and storm mode

The supercellular storms studied herein are dynamically quite different from simple single- or multicellular storms, so comparison of the WK82 and SL16 results to a simpler storm mode is valuable as a further control.

The values of η_m in WK82 and SL16 are substantially smaller than the 0.3–0.8 range of η_m reported by Mansell et al. (2010) in their simulation of a storm with a low flash rate of $\mathcal{O}(1\,\text{min}^{-1})$. Using simulation data from a rerun of that case, we found $\tilde{\mu}_c = 0.050$, or 2.4 times larger than WK82 and 2.6 times larger than SL16.

Each flash in that storm spanned nearly its entire width, a distance of about 6 km. Its small updraft volume (no more than $100\,\text{km}^3$) and low rate of electrification contrasts with the two storms simulated here. However, WK82 had an updraft volume twice that of SL16, so variation in storm volume and electrification rate did not systematically explain the variability in μ_c from case to case. While many prior studies (Schultz et al. 2015; Deierling and Petersen 2008; Dahl et al. 2011b; Basarab et al. 2015) have shown the utility of volumetric storm measures (usually for updraft, graupel, or mixed phase reflectivity volume) in parameterizing the trends in flash rate, updraft volume does not have obvious utility in explaining variability in μ_c.

Clearly, it would be ill advised in future work to assume a universal μ_c, especially if storm volume is not accounted for (Dahl et al. 2011a), since it varies by at least a factor of 10 from storm to storm. The variability in μ_c results in relative errors on the order of 100%. However, such errors are not uncommon in flash rate parameterizations based on thunderstorm kinematic and microphysical proxies (Carey et al. 2019). Nevertheless, it is encouraged that both flash area and storm size may be used in future studies to develop an adaptive μ_c that accounts for these errors, and improves upon energy estimates in different regions of a storm (e.g., convective and anvil). In that light, this

work has established that it is possible to quantify flash energy from lightning mapping observations, with somewhat better than order of magnitude accuracy and having the correct trend, placing it on the same footing as other lightning estimation approaches. The reconstruction of the energy trend in addition to its magnitude is especially valuable for further comparison with meteorological dynamics, as changes to storm state are the essence of practical thunderstorm forecasting.

The experiments here considered the population of flashes for a whole storm. However, it is also known that some regions of large storms have preferentially smaller flashes that are associated with the updraft magnitude and its turbulence intensity (Bruning and MacGorman 2013; Schultz et al. 2015). The relative importance of the correct energy estimates at small flash sizes takes on added importance in these regions, where comparison to the internal meteorological behavior of the storm might also be of interest. While this study has focused on a representative $\tilde{\mu}_c$, the systematic increase of μ_c for smaller flashes (Fig. 8) could be parameterized to further improve energy estimates in these regions, and to account for differences in storm sizes.

To summarize, one of our stated interests is in estimating flash energy ΔW_m (and its total for many flashes) from lightning mapping observations. W_d provides a standalone physical model for flash behavior from which energy estimates can be determined using observables and one parameter, μ_c, that serves as a normalization factor tied to the fraction of energy a discharge removes. When combined with the observation that even a simple total area calculation better matches the energy trend than flash rate (Figs. 2, 3), it seems clear that a total flash energy estimate including flash geometry (area, depth), in addition to flash rate, is a useful approach.

7. Summary and concluding remarks

Flash energy estimates based on a simple electrostatic calculation that utilized flash geometry gave results similar to those found in two numerically simulated storms. Lightning mapping systems can provide flash geometry directly from observations, which offers the possibility of estimating thunderstorm electrostatics in future work. The purpose of this study was to investigate the suitability of a flash-geometry-dependent capacitor model for calculating the electrical energy dissipated by lightning flashes mapped in 3D.

Many applications, from energy trends in individual storms to aggregated flash energy in a climatology, might wish to take the simple route of parameterizing electrical energy on flash rate alone (especially if mapped flash data are not available), on the assumption that any errors in energy are symmetrically distributed across a large population. The flash-size-dependent power-law variability and dependence on storm mode shown herein means that a single, per-flash energy scaling factor, regardless of estimation method, is likely to result in bias due to asymmetry.

Future work may seek to examine if the method used to compute flash areas may have an impact on how W_d captures ΔW_m since it is possible that our method of computing the flash area may introduce error by overgeneralizing both positive and negative channel extents—especially if these channel segments

are spatially offset and do not overlap. It is possible to use an alternative method to calculate flash areas so as to test the impact of how flash size is defined in reference to COMMAS energy values. Therefore, while the geometry-dependent capacitor model and μ_c had some desirable properties that mitigated errors of W_c as demonstrated by positive covariances with ΔW_m, some remained, and future work should be mindful of them.

Energetically, not every flash counts the same, and so parameterization of electrical power on flash rate alone is fraught with error when that error is not symmetrically distributed across a large population. The flash-size-dependent power-law variability and dependence on storm mode shown herein means that a choice of a single, per-flash energy scaling factor, regardless of estimation method, is likely to result in bias. Applications to energy trends in individual storms and aggregated flash energy in climatologies should be mindful of such errors, as well as the additional error that remained in this study when using a geometry-dependent capacitor model.

At the smallest flash sizes, $\mu_c \approx 1$. This result supports our expectation that flash discharge processes are, for smaller flashes, more closely linked to the local energy distribution than to the whole storm. The largest flashes had $\mu_c \ll 1$, because the assumption of constant large electric field within the capacitor volume causes a large overestimate.

In the interest of examining how a capacitor model may be used to predict whole storm and local charging processes separately, and to minimize the flash size dependance on μ_c for retrieval of a universal value that minimizes the errors shown in this work, a subsequent study will examine how the capacitor model (and the adjustment factor μ_c derived in relation to ΔW_m) may be parameterized based on the similarities between the Kolmogorov turbulent energy spectrum and an aggregated flash width-energy dependance identified in Bruning and MacGorman (2013).

This study's refinement of the capacitor model of Bruning and MacGorman (2013) and Bruning and Thomas (2015) is therefore recommended for use with LMA data where no other electrostatic information is available. The wide availability of datasets [e.g., LMA, Geostationary Lightning Mapper (GLM)] that continuously characterize the flash rate and flash geometry raises the prospect for quantifying flash electrostatic energy as a routine element of studies relating thunderstorm processes to lightning.

REFERENCES

Basarab, B. M., S. A. Rutledge, and B. R. Fuchs, 2015: An improved lightning flash rate parameterization developed from

Colorado DC3 thunderstorm data for use in cloud-resolving chemical transport models. *J. Geophys. Res. Atmos.*, **120**, 9481–9499, https://doi.org/10.1002/2015JD023470.

Bitzer, P. M., and Coauthors, 2013: Characterization and applications of VLF/LF source locations from lightning using the Huntsville Alabama Marx Meter Array. *J. Geophys. Res. Atmos.*, **118**, 3120–3138, https://doi.org/10.1002/jgrd.50271.

Boccippio, D. J., 2002: Lightning scaling relations revisited. *J. Atmos. Sci.*, **59**, 1086–1104, https://doi.org/10.1175/1520-0469(2002)059<1086:LSRR>2.0.CO;2.

Borovsky, J. E., 1998: Lightning energetics: Estimates of energy dissipation in channels, channel radii, and channel-heating risetimes. *J. Geophys. Res.*, **103**, 11 537–11 553, https://doi.org/10.1029/97JD03230.

Brothers, M. D., E. C. Bruning, and E. R. Mansell, 2018: Investigating the relative contributions of charge deposition and turbulence in organizing charge within a thunderstorm. *J. Atmos. Sci.*, **75**, 3265–3284, https://doi.org/10.1175/JAS-D-18-0007.1.

Bruning, E. C., and D. R. MacGorman, 2013: Theory and observations of controls on lightning flash size spectra. *J. Atmos. Sci.*, **70**, 4012–4029, https://doi.org/10.1175/JAS-D-12-0289.1.

——, and R. J. Thomas, 2015: Lightning channel length and flash energy determined from moments of the flash area distribution. *J. Geophys. Res. Atmos.*, **120**, 8925–8940, https://doi.org/10.1002/2015JD023766.

Bryan, G. H., J. C. Wyngaard, and J. M. Fritsch, 2003: Resolution requirements for the simulation of deep moist convection. *Mon. Wea. Rev.*, **131**, 2394–2416, https://doi.org/10.1175/1520-0493(2003)131<2394:RRFTSO>2.0.CO;2.

Calhoun, K. M., D. R. MacGorman, C. L. Ziegler, and M. I. Biggerstaff, 2013: Evolution of lightning activity and storm charge relative to dual-Doppler analysis of a high-precipitation supercell storm. *Mon. Wea. Rev.*, **141**, 2199–2223, https://doi.org/10.1175/MWR-D-12-00258.1.

Carey, L. D., E. V. Shultz, C. J. Schultz, W. Deierling, W. A. Petersen, A. L. Bain, and K. E. Pickering, 2019: An evaluation of relationships between radar-inferred kinematic and microphysical parameters and lightning flash rates in Alabama storms. *MDPI Atmos.*, **10**, 796, https://doi.org/10.3390/atmos10120796.

Conner, T., Ed., 1967: The 1967 APRA-AEC joint lightning study at Los Alamos. Los Alamos Science Laboratory Rep., Vol. 1, 32 pp.

Cooray, V., 1997: Energy dissipation in lightning. *J. Geophys. Res.*, **102**, 21 401–21 410, https://doi.org/10.1029/96JD01917.

——, 2014: Power and energy dissipation in negative lightning return strokes. *Atmos. Res.*, **149**, 359–371, https://doi.org/10.1016/j.atmosres.2013.10.017.

Dahl, J. M. L., H. Holler, and U. Schumann, 2011a: Modeling the flash rate of thunderstorms. Part I: Framework. *Mon. Wea. Rev.*, **139**, 3112–3124, https://doi.org/10.1175/MWR-D-10-05031.1.

——, ——, and ——, 2011b: Modeling the flash rate of thunderstorms. Part II: Implementation. *Mon. Wea. Rev.*, **139**, 3112–3124, https://doi.org/10.1175/MWR-D-10-05032.1.

Deierling, W., and W. A. Petersen, 2008: Total lightning activity as an indicator of updraft characteristics. *J. Geophys. Res.*, **113**, D16210, https://doi.org/10.1029/2007JD009598.

Dwyer, J. R., 2003: A fundamental limit on electric fields in air. *Geophys. Res. Lett.*, **30**, 2055, https://doi.org/10.1029/2003GL017781.

Fierro, A. O., and E. R. Mansell, 2017: Electrification and lightning in idealized simulations of a hurricane-like vortex subject to

wind shear and sea surface temperature cooling. *J. Atmos. Sci.*, **74**, 2023–2041, https://doi.org/10.1175/JAS-D-16-0270.1.

Guo, C., and E. P. Krider, 1982: The optical and radiation field signatures produced by lightning return stroke. *J. Geophys. Res.*, **87**, 8913, https://doi.org/10.1029/JC087iC11p08913.

Hill, R. D., 1979: A survey of lightning energy estimates. *Rev. Geophys.*, **17**, 155–164, https://doi.org/10.1029/RG017i001p00155.

Koshak, W., 2021: GLM estimates of LNO_X over the continental United States: Ground and cloud flash differences. *23rd Conf. on Atmospheric Chemistry*, Virtual, Amer. Meteor. Soc., 2A.8, https://ams.confex.com/ams/101ANNUAL/meetingapp.cgi/Paper/379966.

Kuhlman, K. M., C. L. Ziegler, E. R. Mansell, D. R. MacGorman, and J. M. Straka, 2006: Numerically simulated electrification and lightning of the 29 June 2000 STEPS supercell storm. *Mon. Wea. Rev.*, **134**, 2734–2757, https://doi.org/10.1175/MWR3217.1.

Lhermitte, R., and P. R. Krehbiel, 1979: Doppler radar and radio observations of thunderstorms. *IEEE Trans. Geosci. Electron.*, **17**, 162–171, https://doi.org/10.1109/TGE.1979.294644.

MacGorman, D. R., J. M. Straka, and C. L. Ziegler, 2001: A lightning parameterization for numerical cloud models. *J. Appl. Meteor.*, **40**, 459–478, https://doi.org/10.1175/1520-0450(2001)040<0459:ALPFNC>2.0.CO;2.

Maggio, C. R., T. C. Marshall, and M. Stolzenburg, 2009: Estimations of charge transferred and energy released by lightning flashes. *J. Geophys. Res.*, **114**, D14203, https://doi.org/10.1029/2008JD011506.

Malan, D. J., 1963: *Physics of Lightning*. English Universities Press, 176 pp.

Mansell, E. R., D. R. Macgorman, C. L. Ziegler, and J. M. Straka, 2002: Simulated three-dimensional branched lightning in a numerical thunderstorm model. *J. Geophys. Res.*, **107**, 4075, https://doi.org/10.1029/2000JD000244.

——, ——, ——, and ——, 2005: Charge structure and lightning sensitivity in a simulated multicell thunderstorm. *J. Geophys. Res.*, **110**, D12101, https://doi.org/10.1029/2004JD005287.

——, C. L. Ziegler, and E. C. Bruning, 2010: Simulated electrification of a small thunderstorm with two-moment bulk microphysics. *J. Atmos. Sci.*, **67**, 171–194, https://doi.org/10.1175/2009JAS2965.1.

Marshall, T. C., and M. Stolzenburg, 2001: Voltages inside and just above thunderstorms. *J. Geophys. Res.*, **106**, 4757–4768, https://doi.org/10.1029/2000JD900640.

——, ——, C. R. Maggio, L. M. Coleman, P. R. Krehbiel, T. Hamlin, R. J. Thomas, and W. Rison, 2005: Observed electric fields associated with lightning initiation. *Geophys. Res. Lett.*, **32**, L03813, https://doi.org/10.1029/2004GL021802.

Mecikalski, R. M., A. L. Bain, and L. D. Carey, 2015: Radar and lightning observations of deep moist convection across northern Alabama during DC3: 21 May 2012. *Mon. Wea. Rev.*, **143**, 2774–2794, https://doi.org/10.1175/MWR-D-14-00250.1.

Nag, A., and V. A. Rakov, 2010: Compact intracloud lightning discharges: 2. Estimation of electrical parameters. *J. Geophys. Res.*, **115**, D20103, https://doi.org/10.1029/2010JD014237.

Schultz, C. J., W. A. Petersen, and L. D. Carey, 2015: Insight into the kinematic and microphysical processes that control lightning jumps. *Wea. Forecasting*, **11**, 1591–1621, https://doi.org/10.1175/WAF-D-14-00147.1.

Stolzenburg, M., D. W. Rust, B. F. Smull, and T. C. Marshall, 1998: Electrical structure in thunderstorm convective regions 1. Mesoscale convective systems. *J. Geophys. Res.*, **103**, 14 059–14 078, https://doi.org/10.1029/97JD03546.

Vonnegut, B., 1963: Some facts and speculations concerning the origin and role of thunderstorm electricity. *Severe Local Storms*, *Meteor. Monogr.*, Vol. 5, Amer. Meteor. Soc., 224–241, https://doi.org/10.1007/978-1-940033-56-3_11.

Weinheimer, A. J., and A. A. Few, 1987: The electric field alignment of ice particles in thunderstorms. *J. Geophys. Res.*, **92**, 14 833–14 844, https://doi.org/10.1029/JD092iD12p14833.

Weisman, M. L., and J. Klemp, 1982: The dependence of numerically simulated convective storms on vertical wind shear and buoyancy. *Mon. Wea. Rev.*, **110**, 504–520, https://doi.org/10.1175/1520-0493(1982)110<0504:TDONSC>2.0.CO;2.

Wicker, L. J., and R. B. Wilhelmson, 1995: Simulation and analysis of tornado development and decay within a three-dimensional supercell thunderstorm. *J. Atmos. Sci.*, **52**, 2675–2703, https://doi.org/10.1175/1520-0469(1995)052<2675:SAAOTD>2.0.CO;2.

Wiens, K. C., S. A. Rutledge, and S. A. Tessendorf, 2005: The 29 June 2000 supercell observed during the STEPS. Part II: Lightning and charge structure. *J. Atmos. Sci.*, **62**, 4151–4177, https://doi.org/10.1175/JAS3615.1.

Williams, E. R., 1985: Large-scale charge separation in thunderclouds. *J. Geophys. Res.*, **90**, 6013–6025, https://doi.org/10.1029/JD090iD04p06013.

——, and R. M. Lhermitte, 1983: Radar tests of the precipitation hypothesis for thunderstorm electrification. *J. Geophys. Res.*, **88**, 10 984–10 992, https://doi.org/10.1029/JC088iC15p10984.

Wilson, C. T. R., 1920: Investigations on lightning discharges and on the electric field of thunderstorms. *Philos. Trans. Roy. Soc. London*, **221A**, 73–115, https://doi.org/10.1098/rsta.1921.0003.

Wu, T., D. Wang, and N. Takagi, 2018: Lightning mapping with an array of fast antennas. *Geophys. Res. Lett.*, **45**, 3698–3705, https://doi.org/10.1002/2018GL077628.

Zhivlyuk, Y. N., and S. L. Mandel'shtam, 1961: On the temperature of lightning and force of thunder. *Sov. Phys. JEPT*, **13**, 338–340.

Zhu, Y., and Coauthors, 2020: Huntsville Alabama Marx Meter Array 2: Upgrade and capability. *Earth Space Sci.*, **7**, e2020EA001111, https://doi.org/10.1029/2020EA001111.